



Original paper

A Review on Application of Glass Fiber-Reinforced Polymer as a Strengthening Material for Unreinforced Masonry Walls

Mohammad Norouzi Shavir ^{1*}, Mohammadreza Moradi ², Majid Alipoor ³, Reza Sakizadeh ⁴, Peyman Beiranvand ⁵

¹School of Civil Engineering, College of Engineering, University of Tehran, Tehran, Iran.

^{2,4,5} School of Civil Engineering, Iran University of Science and Technology, Narmak, Tehran, Iran.

³Department of Civil Engineering, Khorramabad Branch, Islamic Azad University, Khorramabad, Iran.

ARTICLE INFO

Article history:

Received 17 July 2024

Accepted 10 September 2024

Keywords:

Unreinforced Masonry Wall

GFRP

Theoretical Equations

Cyclic Loading

Strengthening Materials

ABSTRACT

Since the Unreinforced masonry structures are prone to dynamic loadings induced by earthquakes, a thorough comprehension of the behavior of these structures will help to improve their seismic performance. On the other hand, seismic performance improvement of unreinforced masonry walls was a very vast field of investigation. The primary aim of this paper is to study the comparison between the response of the unreinforced and strengthened model. Furthermore, the failure debonding mechanisms of strengthened shear wall models with glass fiber reinforced polymer (GFRP) are discussed. A systematic review of the literature was conducted on the topic with a major focus on the arrangement of the observation used GFRP materials for strengthening techniques, theoretical/analytical prognostication equations formulating the experimental investigations in the research, determination of the progress in the research areas, and identifying the gap in the literature. Eventually, a systematic review of literature will assist in identifying the gap in the knowledge about the Masonry walls reinforced with GFRP and determine the most critical design parameters affecting the structural performance of these types of structures.



DOI: <https://doi.org/10.21859/jces.8149>

©2024 JCES All rights reserved

1. Introduction

Natural disasters e.g., earthquakes are the most serious risk causing tremendous loss of life and property. In general, casualties of human life in earthquakes occur due to the collapse of buildings and non-engineered dwellings. Singlestorey houses are almost always built without the supervision of an experienced engineer and are more likely to be susceptible and suffer damage during a seismic event. Generally, these types of houses are usually adequate for withstanding the gravity loads and make almost acceptable performance under compression tension. But on the antithesis, these types of structures are grossly inadequate to withstand the lateral inertia loads imposed by earthquakes. According to [1] about 75% of the fatalities attributed to earthquakes are caused by the collapse of buildings

and the greatest proportion is from the collapse of masonry buildings. On the other hand, Masonry structures are widespread in many regions of the world and masonry units of construction still remain as a major building material in many places, especially in rural areas. Approximately 60% of people in the whole world are living in masonry buildings that are made by piling up bricks, sun-dried mud bricks (Also known as adobe), stone and concrete blocks. [2] A large percentage of these buildings are currently associated with low economic resources. Furthermore, a large portion of the existing earth constructions is now located in regions where seismic hazards cannot be neglected. Therefore, structural strengthening methods were carried out and different techniques are often necessary to allow unreinforced masonry buildings to remain in the future. Structural

*Corresponding author Email: peyman51471366@gmail.com

retrofitting of Masonry structures are developed to increase structural capacity or to control structural damage of unreinforced masonry walls by affecting failure mechanisms and preventing a cracking pattern. [3] When a masonry structure is exposed to loading, load-bearing walls are mainly subjected to two types of possible failure mechanisms such as in-plane shear and out-of-plane bending [4, 5]. According to Iuorio et al. [6] In general, the out-of-plane failure of URM walls is divided by either one-way or twoway bending of the walls. The failure mechanism of masonry buildings can be local or global and can result in a partial or total collapse of the wall. One solution to overcome the out-of-plane failure is to be restrained by providing externally strengthening elements such as proper wall diaphragm connection or I-shaped flanges that supply adequate stiffness [7]. The principal in-plane mechanisms are generally characterized by the following failure modes: 1) shear failure, 2) sliding failure, 3) rocking failure, and 4) toe crushing failure. Among them and with an aspect ratio lower than 1, shear and sliding failure are the most common and general modes of failure observed in URM buildings [8]. The rocking failure is the most ductile failure and the least harmful; sliding shear failure is the least frequent, whereas the diagonal shear failure is the worst type of wall failure since it is very brittle and sudden. [9] Fiber-reinforced polymer (FRP) has become an extensively used popular material to strengthen masonry walls and structures in the past few decades. High strength-to-weight ratio, high initial stiffness, linear elastic behavior, and convenience in the application have made it a material of good choice for the seismic retrofitting and strengthening of the masonry structure. The glass fiber-reinforced polymer (GFRP) sheets were used in tremendous investigations to reinforce masonry walls, it offers significant advantages since the fibers can be externally bonded to the surface without affecting the aesthetics of the structure. Also, it could improve the strength and ductility of the structure. This paper describes an experimental investigation and theoretical study of in-plane shear strengthening using glass-fiber-reinforced polymer (GFRP) as a strengthening material. Using GFRP sheets, bars, and GFRP as a polymer in fiber-reinforced concrete for partially grouting the surface of masonry walls is a typical suggestion of authors. The strengthening could be applied on Only one side or both sides of the masonry wall, each approach has its own benefits and defects, e.g., single-sided strengthening could be more economical and allows the façade of a building to be left untouched.

2. Methodology

Many different strategies for the prediction of the behavior of masonry walls to calculate strength were offered by the authors. Also, regarding retrofitting methods, different techniques to strengthen the new or rehabilitate the existing masonry buildings are presented by scholars. To accomplish the methodical review, relevant studies were identified by searching electronic databases (including Science Direct, Scopus, Web of Knowledge, and Civil Engineering database (ASCE)) for published literature up to May 1st, 2022. More than 50 works were filtered, studied, and classified in this category. In addition, the reference lists of relevant studies were double-checked for reports of other potentially relevant studies. scholar's Studies were eligible if they (1) proposed an equation to anticipate the behavior of URM or retrofitted wall (2) the analytical equation performed in another study and other scholars used this as a reference (3) Regarding strengthening method, assessment of strengthening solutions by performing material and mechanical characterization tests; (4) verified by information regarding the strengthening materials and methodology is provided and (5) were published in English. In fact, it was considered valuable to include these works due to the highly eligible and numerous acceptable information concerning this topic.

3. Analytical Equations for In-Plane Loading

3.1. Single-sided diagonal strips

Capozucca and Magagnini (2020) [10] conducted an experimental investigation via analytical equations to evaluate the In-plane seismic behavior of the 1:3rd single-story historic solid clay brick wall, strengthened on one side, by diagonal GFRP strips. Both of the specimens were subjected to precompression to simulate actual loading conditions in masonry buildings and tested under cyclic lateral loading. (Fig.1)The first one strengthened after damage with EB GFRP strips - and then once again - subjected to the same loading until failure; the Second one was strengthened with GFRP strips without damage and subjected to the same path of loading until failure. The specimens are shaped in double T-shaped sections. The choice of using double T shape sections was attributed to avoid bending

cracking at the base of the wall model, consequently, the failure is initiated only due to shear.



Fig 1. Wall surface with application of the two-component primer (Capozucca and Magagnini [10]).

During the cyclic loading, the loss of strength of the FRP-masonry joint hybrid system can occur in various conditions, e.g., detachment of the composite material, along the surface of the wall material and the adhesive; at the contact between the thin layer of adhesive and the composite and finally, it can occur inside the same composite layer also known as an interlaminar failure.[11] Experimental investigations suggest that one of the failure modes of FRP reinforced masonry joints is delamination failure occurring at a plane located a few millimeters from the surface of the masonry. As known, the ultimate load of strengthening with EB GFRP strips depends strongly on the fracture energy, G_f , which can be evaluated by shear stress-slip laws. The authors proposed different equations to evaluate the fracture energy in unreinforced masonry walls. Due to the lack of generally accepted values for masonry components, missing material properties are calculated based on expressions used in concrete. Walraven and Van der Horst [12] proposed the equation for the tensile strength which was derived from the flexural strength:

$$f_t = f_f \frac{0.06h^{0.7}}{1+0.06h^{0.7}} \tag{1}$$

Where h is the height of the specimen tested in three-point bending. The compressive fracture energy is calculated according to the equation proposed by (Drougkas et al, 2015) [13]:

$$G_f^c = f_c d \tag{2}$$

Where $d = 1 \text{ mm}$. The tensile fracture energy in N/mm is calculated according to the equation proposed by (Drougkas et al., 2019) [14]:

$$G_f^c = 0.073 f_c^{0.18} \tag{3}$$

With the compressive strength f_c from cubic compression test and is in N/mm^2 .

An analytical method to predict the bond capacity of Externally Bonded GFRP-strips on brick masonry walls, considering a simplified elastic model and also has been developed with the presumption that GFRP strips as the adherent material subjected to both axial and shear deformations. [15] The width, thickness, Young ' s modulus, and shear modulus of the intermediate layer are mentioned by b_m , t_m , E_m , and G_m , respectively; the adherent superficial layer with thickness t_1 and the ideal intermediate element of thickness t_m are supposed to be an elastic material. To obtain the maximum value of the interfacial fracture energy, G_f , i.e., the total external energy supply per unit of area required to create delamination along the GFRP strip-to brickwork masonry bonded joint:

$$G_f = \frac{P^2}{2b_1^2 E_1 t_1} \tag{4}$$

The value of load capacity, P , is the superficial glued layer of the GFRP strip, and b_1 , t_1 , and E_1 are respectively the widths, the thickness, and Young ' s modulus of the adherent superficial layer. Although masonry can carry out the main part of compression load for its greater thickness, also GFRP strip is subjected to a part of compression. Cappozucca [17] in another study assessed an investigation on unreinforced double-leaf masonry wall models built with historic solid clay bricks on a 1:3rd scale. The unreinforced models were tested under combined compression and

shear loading. After damage they were strengthened with two types of external bonded composite materials - diagonal Glass-FRP strips and steel fiber reinforced cement grout (SRG) - and then once again subjected to the same loading until failure. Under compression by alternative horizontal force, strengthening with SRG strips has shown a weak behavior. A theoretical model which may be used to analyze the buckle response is described. Internal energy contributions due to bending of the ideal beam and to the response of springs for the displacement $y(x)$ are as follows:

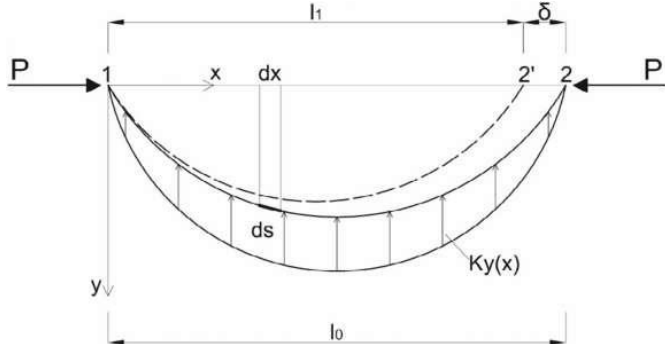


Fig 2. Beam model for strip on elastic springs under compression. Cappozucca [17].

This compression leads to Delamination buckling becoming the damage of the strengthening glued to the masonry surface and causing a major failure mechanism. GFRP strip is assumed as an elastic beam embedded subjected to compressive forces at the ends. The strip may buckle under a system of loads, P, due to compressive forces and load reactions, q, of ideal springs with constant k. (Fig.2) According to the energy method following the Rayleigh's procedure, the constant k depends on the width b1 of strips by the relation $k=k_0 \cdot b1$ and the critical buckling load determined by energy method may be determined as it follows: [16]

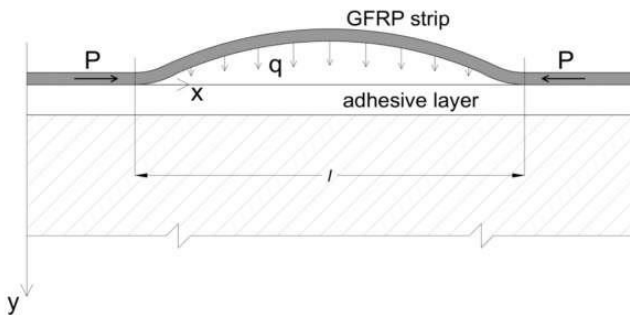


Fig 3. Model to analyze the delamination buckling of GFRP strip (Capozucca and Magagnini (2020) [10]).

The primary impact of the strengthening method was the failure of the walls retrofitted with GFRP strips that occurred with the cracking of the masonry and the failure of the GFRP strips after the local loss of bond. Furthermore, the strengthening of the GFRP strips led to an increase in deformation energy due to wider load cycles. The strengthening of the GFRP equipped panels led to an increase in resistance, however, what is mainly observed is a strong increase in lateral deflection with an increase in ductility. Furthermore, failure of the GFRP reinforced panels occurred with cracking of the masonry and the resulting failure of the GFRP strips due to detachment. Most importantly, the retrofitting of the GFRP-equipped panels led to an increase in deformation energy due to wider load cycles. A local phenomenon of instability of the strengthening can cause brittle failure resulting from debonding mechanism. Consequently, Although GFRP causes an increase in resistance and reveals a major displacement capacity, Cappozucca [17] results focus attention on a need that the use of composite GFRP material generally does not satisfy the retrofitting method by itself.

4. Analytical Equations for Out-of-Plane Loading

4.1. Brick masonry wallet reinforced by GFRP strips

Sistani nezhad and Kabir [47] carried out experimental study on behavior of masonry wallets strengthened by GFRP strips with different

reinforcement ratio and configurations e.g., diagonal, grid and combination of grid and diagonal. (Fig. 4)

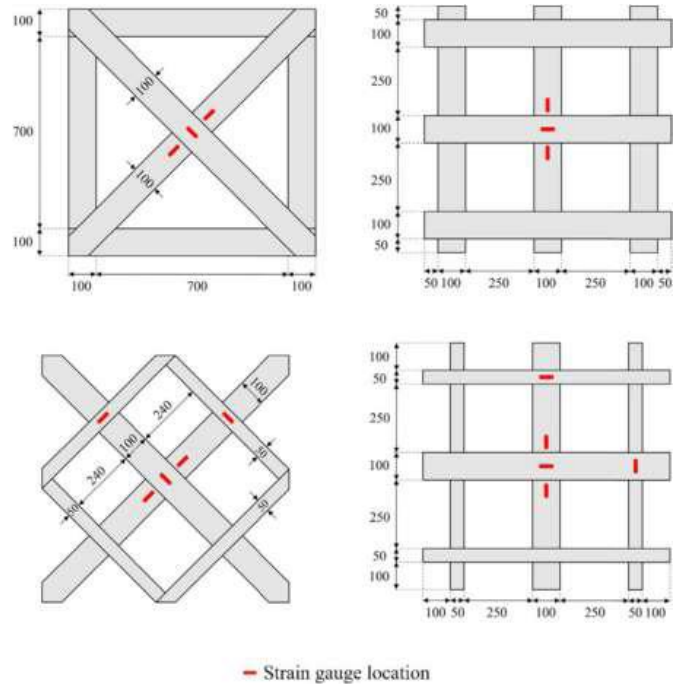


Fig 4. Configuration of strengthening and location of strain gauges (Sistani Nezhad and Kabir [47]).

The results were compared in the terms of laid carrying capacity, displacement, and energy absorption and failure mode. In total six double-wy the wallets with nominal dimension of 880 x 880mm were built and subjected to out-of plane vertical monotonic loading. In retrofitted masonry wallets, the out-of-plane loading in general caused shear and bending failure. In stark contrast, however, the unreinforced masonry wallet failure was due to spreading cracks through mortar joints on the tension side of the wallet. Longitudinal curvature formation caused an elevation of four corners. Due to the significant ductility by strengthening method considerable curvature is observed in strengthened specimens. Also, out-of-plane strength of retrofitted specimens was higher than the control wall. For the reference specimen at the elastic phase, the lateral load is proportional to the lateral deformation up to 0.73mm displacement. The ultimate load is reached to 11.68kN with 1.06mm out-of-plane deformation. The ultimate out-of-plane deformation at the collapsed state is obtained at 8.3mm. In contrast, the wallet strengthened by a layer of cement on both sides is considerably higher. The ultimate load and its corresponding displacement are measured as 25.67kN and 2.3mm, respectively. These values are 120% and 117% higher than that of the unreinforced wall, correspondingly. Also dissipates 130.9kNm energy that is 386.6% more than the control specimen. But due to the sharp dropping of carrying the load after the peak value, in general, post peak behavior of this specimen tends to be brittle and sudden collapse. The behavior of the wallet with reinforcement ratio (longitudinal FRP area to the cross-section area) of approximately 0.269%, is approximately linear up to 1.29mm displacement. Ultimate strength is about 43.5kN with the out-of-plane displacement of 2.56mm. In this case, the specimen's out-of-plane strength is increased about 272% with a corresponding displacement of 141% more than the unreinforced specimen. Wall with the reinforcement ratio of 0.237%, carries a maximum load of 82kN with a corresponding mid-span displacement of 7.49mm. The out-of-plane strength and corresponding displacements are 602% and 607% of the control wall, respectively. The overall failure is induced by detachments of GFRP strips and then the load is plunged and the crack propagation is extended through the masonry wall surface. The primary behavior wallet with reinforcement ratio of 0.168% at the load-deflection curve is linear up to the 20.5kN and 1.14mm displacement. It extended to the ultimate load 42.04kN with the corresponding displacement of 2.75mm. At this point, the failure considerably occurred by crushing of masonry in compression causing

decrease of carrying the load. The failure mechanism was due to the weak bond between adhesive and substrate delamination of strips. The ultimate capacity and the corresponding displacements are 260% and 159% as compared to the corresponding values in control specimens, respectively. A wall with reinforcement ratio of 0.158% is linear until the onset of micro cracks in the tension side of the wall before functioning of FRP action. This point belongs to the displacement of 1.04mm under a load of 20.14kN the ultimate load reaches to 51.26kN at 4.22mm out-of-plane displacement. In comparison to the 4th retrofitted specimen to the reference wall the strength soars to 338% higher than unreinforced masonry wallet. Ductility is calculated by dividing ultimate deformation at 80% of load carrying capacity to yield deformation where the first reduction in stiffness occurs. In each retrofitted specimen by GFRP strips the improvement in the displacement ductility ratio is 55%, 53%, 41% and 40% of different patterns of GFRP reinforcements and reinforcement ratio. GFRPs strips that are applied partially on the masonry facades can considerably improve the ductility of force-displacement response and energy absorption under

monotonic loading. Furthermore, by applying partially GFRP strips on the tension side of masonry walls great improvement in out-of-plane strength is achieved. Ultimate bending moment and out-of-plane strength capacity of the masonry cross section is defined by considering three different failure modes; FRP debonding, FRP rupture and the compressive crushing of masonry. Since FRP debonding mode does not occur as the main failure mechanism, analytical equations are defined for the compressive crushing of masonry and FRP rupture. Therefore, the depth of compressive part can be determined.

5. Results

In this section, a comparison between the experimental results of different authors on the improvement of the seismic performance of unreinforced masonry walls with GFRP materials were provided. To have a better analogy, all studies with different conditions of dimension, geometry, loading procedures and different application technique of strengthening were reported and the results were compared.

Table 1. Database of experimental programs based on GFRP retrofitting technique.

Authors	Type of Masonry	Type of Loading	Length (mm)	Height (mm)	Retrofit method	Details of strengthening method	Contribution of Strengthening	Failure mode
Del Zoppo et al. [25]	Tuff bricks	Diagonal Compression	1200	1200	GFRP Grid and Cementitious Matrix	Single side; double side	Increase in shear capacity, single side: 42-85%; Both side: 138- 288%	Sudden failure changes to uniform cracking and ductile post-peak behaviour
Capozucca and Magagnini (2021) [23]	Clay brick	Cyclic shear test	850	633	GFRP Strips	Diagonal and Horizontal	Shear capacity increased by 50%	GFRP detachment
Capozucca and Magagnini (2020) [10]	Clay brick	Cyclic Shear test	835	633	GFRP Strips	Diagonal	Failure mode occurs at F:50 kN, F:55 kN change to F: 92.2 kN	Detachment and Buckling of GFRP strips
Cappozucca [17]	Clay brick	Cyclic shear test	840	633	GFRP / SRG strips	Diagonal	Ductility increased, - 1.2 to - 3.7mm; 0.8 to 1.25mm	Debonding of GFRP strips and buckling of SRG
Stratford et al. [18]	Clay brick and concrete block	Static shear test	1200	1200	GFRP sheet	Single-side strengthening	Load capacity; Clay: 115 to 190 kN (65%) Concrete: 80 to 110 and 130 kN (38 and 83%)	Debonding of GFRP
Yu et al. [28]	Concrete block	Diagonal cyclic test	1630	1630	GFRP bars	Prestressed NSM GFRP bars	Maximum shear stress: 0.62 to 1.34 MPa High stress cement layer: P: 120% δ_{max} : 117%	Diagonal cracks change to combination of shear friction and shear sliding
Sistani Nezhad and Kabir [47]	Clay brick	Out-of-plane loading	880	880	GFRP strips	Different Reinforcement Ratio	P: 272% δ_{max} : 141% 0.237% P: 602% δ_{max} : 607% 0.168% P: 260% δ_{max} : 159%	Crushing at the compressive area and rupture of tensile GFRP
Gattesco	Cobble	Four points	1000	3000	GFRP mesh	Both side mortar coating	Bending moment capacity: 4-5	Cracks in middle third of wall

and Boem (2017) [48]	stone	bending				with GFRP mesh		times; deflection: 25 times	caused GFRP wire failure
Dong et al. [49]	Clay brick	Four points bending	235	870	Glass textile	TRM with addition of PVA fibres to matrix		Peak loads increased 12.6 times; ductility factor: 2.66 times	In the constant moment region bed joint between brick and mortar debonded
Abdulsalam et al. [50]	Clay brick	Out-Of-Plane loading	460	1420	GFRP Sheet	Sheets anchored		Load carrying capacity increased by 100%	Due to GFRP anchor Spike rupture of GFRP sheet occurred
Tumialan et al. [52]	Clay brick	Out-Of-Plane Loading	In- Situ		GFRP Laminate	Application of GFRP laminate directly to masonry wall compared to without removal of plaster		Retrofitted over plaster increased 17% in load capacity; without plaster increased by 40 %	Arching mechanism due to flexural cracks
Borri et al. [40]	Stone masonry; Pebble masonry	Cyclic diagonal test	1200	1200	GFRM, Steel mesh as a Hybrid	GFRP mesh jacketing and mortar coating		Shear strength: GFRM: Stone: 17% pebble: 40% Hybrid: Stone: 87% Pebble: 112% Resistance Solid brick and rubble stone: 70 and 90% Cobble stone (strong mortar): 220% weak mortar: 350% Ductility: 1.7 to 8 times	Diagonal crack instead of concentrating in middle widespread on the surface
Gattesco and Boem (2015) [41]	1-brick 2-Rubble 3-Cobble	Diagonal Compression	1160	1160	GFRP mesh and Mortar coating	Both side mesh jacketing and mortar coating		Maximum load on both side; single side and hybrid: 155kN to 216, 188 and 201 kN, ductility: 11.9mm to 22.72, 14.08 and 24.08mm	Linear diagonal cracks
Gattesco et al. [42]	Stone masonry	Lateral Cyclic	1500	2000	GFRP mesh with mortar coating	Hybrid one side GFRP and other steel-strands		Lad capacity and stiffness was 215.6 kN and 4829 MPa (7 and 18.4 % increase)	Single side: out of plane bending caused failure, both side and hybrid detachment of reinforced coating
Borri et al. [43]	Clay brick	Diagonal cyclic	300	300	GFRP grids	Grids inserted to thermal insulation jacketing			Diagonal cracks along the compressed diagonal axes

Mustafaraj and Yardim [45]	Clay brick	Diagonal compression	1200	1200	GFRP mesh	GFRP mesh embedded mortar jacketing in both side	Shear resistance 127% ductility: 1100% modulus of rigidity: 650% Dissipation of energy increased in 100 to 286.5% ultimate displacement grow from 100 to 166.4%	Linear diagonal cracks with moderate post-peak behaviour Brick at footing crushed detachment of GFRP sheets	
Weng et al. [46]	Clay brick	Lateral cyclic test	3000	1500	GFRP mesh	Cement mortar coating on GFRP mesh	Grid and Ladder shape GFRP mesh used in bed joints	Lateral capacity increased in average 54.7% (grid 85% ladder: 25%) Failure mode occurred at increased capacity and ductility, strength: 27-32%, Dissipation of energy: 33-85% Ultimate strain in boring: 23-43% and grooving method: 21.3-33% increased	Grid: detachment of mortar a sliding, Ladder: diagonal step failure Failure due to the diagonal shear cracks
Sadek and Lissel [53]	Hollow concrete block	Lateral cyclic test	1600	1400	GFRP Geogrids	Grid and Ladder shape GFRP mesh used in bed joints	Ferrocement: Laying of mortar layer and diagonal GFRP sheets	Failure mode occurred at increased capacity and ductility, strength: 27-32%, Dissipation of energy: 33-85% Ultimate strain in boring: 23-43% and grooving method: 21.3-33% increased	Failure due to the diagonal shear cracks
El-Diasity et al. [54]	Clay brick	Lateral cyclic test	2400	2020	GFRP Ferrocement	Ferrocement: Laying of mortar layer and diagonal GFRP sheets	Boring and Grooving methods in mounting the sheets	Strengthened wall remain attached to Infill	Failure due to the diagonal shear cracks
Eftekhari and Emami [22]	Clay brick	Diagonal compression	870	870	GFRP sheets	GFRP sheets attached to one side of wall and anchored infill	Boring and Grooving methods in mounting the sheets	Strengthened wall remain attached to Infill	Sliding in horizontal bed joints and diagonal splitting
Al Sayed et al. [55]	Hollow concrete block	Blast loading	2900	1500	GFRP sheets	GFRP sheets attached to one side of wall and anchored infill	Boring and Grooving methods in mounting the sheets	Strengthened wall remain attached to Infill	Debonding of GFRP sheets observed

Based on the investigation of the literature concerning experimental tests on unreinforced masonry walls and GFRP strengthened masonry wall, a dataset of the results of shear-compression tests and out-of-plane test has

been built and the main data are listed in Table 2. Note that in the last column DT, DB, DL and SF are shortened words for diagonal tension, debonding, delamination and Shear failure.

Table 2. Database of experimental results on masonry walls reinforced by GFRP.

Authors	Set	Specimen	Description	Type of loading	Length (L) (mm)	Height (H) (mm)	Aspect ratio (H/L)	P_{max} [kN]	P_u [kN]	δ_{max} [mm]	δ_u [mm]	μ	Failure mode
								or f_{max} [MPa]	or f_u [MPa]	or γ_{max} [%]	or γ_u [%]		
Del zoppo et al. [25]	1	URM1	Unreinforced masonry wall	Diagonal compression	1200	1200	1	131 kN; 0.31 MPa	0.31 MPa	0.08 %	0.08 %	1.00	DT
		URM2		Diagonal compression	1200	1200	1	100 kN; 0.24 MPa	0.24 MPa	0.11 %	0.11 %	1.00	DT
		URM3		Diagonal compression	1200	1200	1	98 kN; 0.23 MPa	0.23 MPa	0.05 %	0.05 %	1.00	DT
		URM4		Diagonal compression	1200	1200	1	96 kN; 0.23 MPa	0.23 MPa	0.09 %	0.17 %	1.89	DT
		URM5		Diagonal compression	1200	1200	1	122 kN; 0.3 MPa	0.3 MPa	0.09 %	0.11 %	1.22	DT
		URM6		Diagonal compression	1200	1200	1	93 kN; 0.23 MPa	0.23 MPa	0.14 %	0.15 %	1.07	DT
	2	SC-2-1	Sand-Cement Plaster	Diagonal compression	1200	1200	1	425 kN; 1 MPa	0.9 MPa	0.52 %	0.61 %	1.17	DT+DB
		SC-2-2		Diagonal compression	1200	1200	1	410 kN; 0.94 MPa	0.94 MPa	0.36 %	0.36 %	1.00	DT+DB
	3	SCI-1-1	Cement - lime+ glass fiber plaster on each and both side	Diagonal compression	1200	1200	1	203 kN; 0.48 MPa	0.39 MPa	0.23 %	0.64 %	2.78	DT
		SCI-1-2		Diagonal compression	1200	1200	1	202 kN; 0.48 MPa	0.39 MPa	0.37 %	0.79 %	2.14	DT
		SCI-2-1		Diagonal compression	1200	1200	1	401 kN; 0.95 MPa	0.9 MPa	0.38 %	0.45 %	1.18	DT+DB
		SCI-2-2		Diagonal compression	1200	1200	1	378 kN; 0.9 MPa	0.85 MPa	0.09 %	0.24 %	2.67	DT+DB
	4	SL-1-1	lime+ glass fiber plaster on each and both side	Diagonal compression	1200	1200	1	190 kN; 0.45 MPa	0.38 MPa	0.39 %	1.05 %	2.69	DT
		SL-1-2		Diagonal compression	1200	1200	1	185 kN; 0.44 MPa	0.37 MPa	0.19 %	1.36 %	7.16	DT
		SL-2-1		Diagonal compression	1200	1200	1	289 kN; 0.68 MPa	0.7 MPa	0.06 %	0.08 %	1.33	DT+DB
		SL-2-2		Diagonal compression	1200	1200	1	355 kN; 0.83 MPa	0.81 MPa	0.16 %	0.24 %	1.50	DT+DB
	5	G30CL-1-1	GFRP mesh 30*30 with cement - lime mortar + glass fiber on one side and both side	Diagonal compression	1200	1200	1	159 kN; 0.38 MPa	0.3 MPa	0.22 %	0.58 %	2.64	DT
		G30CL-1-2		Diagonal compression	1200	1200	1	156 kN; 0.37 MPa	0.31 MPa	0.66 %	1.75 %	2.65	DT
		G30CL-2-1		Diagonal compression	1200	1200	1	402 kN; 0.95 MPa	0.89 MPa	0.12 %	0.51 %	4.25	DT+DB
		G30CL-2-2		Diagonal compression	1200	1200	1	398 kN; 0.93 MPa	0.76 MPa	0.32 %	0.39 %	1.22	DT+DB
	6	G30L-1-1	GFRP mesh 30*30 with lime mortar + glass fiber on one side and both side	Diagonal compression	1200	1200	1	175 kN; 0.41 MPa	0.36 MPa	0.24 %	0.78 %	3.25	DT
		G30L-1-2		Diagonal compression	1200	1200	1	212 kN; 0.48 MPa	0.4 MPa	0.07 %	0.71 %	10.14	DT
		G30L-2-1		Diagonal compression	1200	1200	1	306 kN; 0.72 MPa	0.59 MPa	0.09 %	0.24 %	2.67	DT+DB
		G30L-2-2		Diagonal compression	1200	1200	1	217 kN; 0.52 MPa	0.42 MPa	0.06 %	0.1 %	1.67	DT+DB
7	G40CL-1-1	GFRP mesh 40*40 with cement - lime mortar + glass fiber on one side and both side	Diagonal compression	1200	1200	1	161 kN; 0.38 MPa	0.32 MPa	0.27 %	0.69 %	2.56	DT	
	G40CL-1-2		Diagonal compression	1200	1200	1	166 kN; 0.39 MPa	0.31 MPa	0.2 %	0.88 %	4.40	DT	
	G40CL-2-1		Diagonal compression	1200	1200	1	448 kN; 1.05 MPa	0.97 MPa	0.76 %	1.81 %	2.38	DT+DB	
	G40CL-2-2		Diagonal compression	1200	1200	1	420 kN; 0.98 MPa	0.83 MPa	0.5 %	0.83 %	1.66	DT+DB+DL	
8	G40L-1-1	GFRP mesh 40*40 with	Diagonal compression	1200	1200	1	163 kN; 0.39 MPa	0.31 MPa	0.2 %	0.66 %	3.30	DT	
	G40L-1-2		Diagonal compression	1200	1200	1	165 kN; 0.39 MPa	0.31 MPa	0.47 %	0.92 %	1.96	DT	

8	G40L-2-1	lime mortar + glass fiber on one side and both side	Diagonal compression	shear	1200	1200	1	314 kN;	0.57	0.07 %	0.34 %	4.86	DT+DB	
	G40L-2-2				Diagonal compression	1200	1200	1	436 kN;					0.69
Capozucca and Magagnini (2021) [23]	1	W1	URM	Cyclic test	shear	850	633	0.74	62.1 kN	55.89 kN	0.6 mm	3.39 mm	5.65	DT
				Cyclic test	shear	850	633	0.74	60.21 kN	54.19 kN	1.94 mm	3.97 mm	2.05	DT
	2	W1-D-GFRP	Wall retrofitted by diagonal GFRP	Cyclic test	shear	850	633	0.74	92.22 kN	83.0 kN	0.81 mm	6.03 mm	7.44	DL
				Cyclic test	shear	850	633	0.74	91.32 kN	82.19 kN	2.1 mm	12.76 mm	6.08	DL
3	W2-H-GFRP W3-H-GFRP	Wall retrofitted by horizontal GFRP	Cyclic test	shear	850	633	0.74	88.76 kN	79.88 kN	2.52 mm	9.37 mm	3.72	DL	
			Cyclic test	shear	850	633	0.74	88.76 kN	79.88 kN	2.52 mm	9.37 mm	3.72	DL	
Sadek and Lissel [53]	1	Wall-C	URM	Cyclic test	shear	1600	1400	0.875	60 kN	40.21 kN	2 mm	5.04 mm	2.52	Step cracks
				Cyclic test	shear	1600	1400	0.875	68 kN	57.39 kN	3 mm	4.05 mm	1.35	Sliding
	3	Wall-G(grid) Wall-G(ladder)	GFRP mesh with sectional area of 7.1 in bed joints	Cyclic test	shear	1600	1400	0.875	105 kN	48.26 kN	5 mm	10.14 mm	2.03	Sliding
				Cyclic test	shear	1600	1400	0.875	96 kN	47.17 kN	5 mm	10.14 mm	2.03	Step cracks
	4	Wall-E(ladder) Wall-E1(Grid) Wall-E2(grid)	GFRP mesh with sectional area of 4.5 in bed joints	Cyclic test	shear	1600	1400	0.875	70 kN	32.17 kN	4 mm	10.14 mm	2.54	Step cracks
				Cyclic test	shear	1600	1400	0.875	111 kN	29.13 kN	10 mm	20.22 mm	2.02	Sliding
	1	CLY-S-CTRL	URM	Lateral Cyclic	shear	2400	2020	0.84	290 kN	248.83 kN	8.5 mm	15.4 mm	1.81	SF-DT
					shear	2400	2020	0.84	360 kN	281.4 kN	7.5 mm	15.1 mm	2.01	SF-DT
2	CLY-S-Ferro-C CLY-S-Ferro-X CLY-S-Ferro-F	Solid masonry wall retrofitted by ferrocement	Lateral Cyclic	shear	2400	2020	0.84	378.5 kN	332.56 kN	11.25 mm	14.05 mm	1.25	Rocking	
				shear	2400	2020	0.84	376 kN	351.16 kN	8.5 mm	11.95 mm	1.41	Rocking	
3	CLY-S-GFRP-X CLY-S-GFRP-F	Solid masonry wall retrofitted by GFRP	Lateral Cyclic	shear	2400	2020	0.84	386 kN	360.46 kN	11 mm	13.8 mm	1.25	Rocking	
				shear	2400	2020	0.84	540 kN	542 kN	14 mm	14 mm	1.00	Rocking	
4	CLY-P-W CLY-P-D	URM with opening	Lateral Cyclic	shear	2400	2020	0.84	250 kN	217.5 kN	12 mm	16.2 mm	1.35	SF	
				shear	2400	2020	0.84	205 kN	120.37 kN	15 mm	27 mm	1.80	SF	
5	CLY-D-Ferro CLY-W-Ferro	URM with opening retrofitted by ferrocement	Lateral Cyclic	shear	2400	2020	0.84	270 kN	185.19 kN	16 mm	34 mm	2.13	Diagonal cracks around opening	
				shear	2400	2020	0.84	335 kN	257.5 kN	7.3 mm	27 mm	3.70	Diagonal cracks around opening	
Gattesco et al. [42]	1	MSR1	URM	Lateral Cyclic	shear	1500	2000	1.33	155 kN	76 kN	7.87 mm	11.9 mm	1.51	DT
				Lateral Cyclic	shear	1500	2000	1.33	216 kN	94 kN	14.98 mm	22.77 mm	1.52	DB
	2	MSR3	GFRM jacketing	Lateral Cyclic	shear	1500	2000	1.33	181 kN	112.5 kN	20.05 mm	24.04 mm	1.20	Out-Of-Plane bending
				Lateral Cyclic	shear	1500	2000	1.33	201 kN	67.5 kN	16.1 mm	24.08 mm	1.50	DB
3	MSR4	Hybrid	Lateral Cyclic	shear	1500	2000	1.33	201 kN	67.5 kN	16.1 mm	24.08 mm	1.50	DB	
		35-UR		Diagonal Cyclic	shear	300	300	1	204.5 kN;	0.28	0.248 %	2.68 %	10.81	DT
								0.753	MPa					

Borri et al. [43]	1	36-UR	URM	Diagonal Cyclic	300	300	1	197.7 kN; 0.702 MPa	0.56 MPa	0.292 %	2.99 %	10.24	DT	
	2	31-RO	Masonry panels retrofitted by GFRP and different mortar coating	Diagonal Cyclic	300	300	1	202.9 kN; 0.69 MPa	0.43 MPa	0.37 %	12.64 %	34.16	DT	
		32-RO		Diagonal Cyclic	300	300	1	228.3 kN; 0.7 MPa	0.45 MPa	0.37 %	9.09 %	24.57	DT	
		33-D		Diagonal Cyclic	300	300	1	236.4 kN; 0.82 MPa	0.75 MPa	0.57 %	7.88 %	13.82	DT	
		34-D		Diagonal Cyclic	300	300	1	258.5 kN; 0.91 MPa	0.66 MPa	0.63 %	12.48 %	19.81	DT	
		37-R2		Diagonal Cyclic	300	300	1	315.6 kN; 1.28 MPa	1 MPa	0.75 %	7.64 %	10.19	DB	
		38-R2		Diagonal Cyclic	300	300	1	325.5 kN; 1.34 MPa	1.02 MPa	0.76 %	7.18 %	9.45	DB	
		39-C		Diagonal Cyclic	300	300	1	431.4 kN; 1.54 MPa	1.25 MPa	0.76 %	11.37 %	14.96	DB	
		40-C		Diagonal Cyclic	300	300	1	420.3 kN; 1.47 MPa	1.19 MPa	0.52 %	6.55 %	12.60	DB	
Mustafaraj and Yardim [45]	1	W1	URM	Diagonal Compression	1200	1200	1	189.31 kN; 0.445 MPa	0.445 MPa	0.06 %	0.06 %	1.00	SF+ Sliding	
	2	W2		Diagonal Compression	1200	1200	1	199.28 kN; 0.47 MPa	0.47 MPa	0.023 %	0.023 %	1.00	SF+ Sliding	
		W3		Diagonal Compression	1200	1200	1	149.46 kN; 0.41 MPa	0.41 MPa	0.04 %	0.04 %	1.00	SF+ Sliding	
		W4-GFRP		Diagonal Compression	1200	1200	1	278.99 kN; 0.6 MPa	0.6 MPa	0.04 %	0.2 %	5.00	DT + yielding of mesh	
	2	W5-GFRP		GFRP mesh embedded in coating	Diagonal Compression	1200	1200	1	209.24 kN; 0.52 MPa	0.52 MPa	0.44 %	0.5 %	1.14	DT + yielding of mesh
		W6-GFRP		Diagonal Compression	1200	1200	1	189.316 kN; 0.44 MPa	0.44 MPa	0.1 %	0.2 %	2.00	DT + yielding of mesh	
Capozucca and Magagnoli (2020) [10]	1	U-W1	Unreinforced masonry wall	Cyclic shear test	835	63	0.74	61.8 kN	46.8 kN	3.36 mm	4.61 mm	1.37	DT	
	2	DR-W1	Reinforced by GFRP strips	Cyclic shear test	835	63	0.74	90.8 kN	78.76 kN	2.98 mm	4.67 mm	1.57	DL	
	3	R-W2	Repaired with GFRP strips	Cyclic shear test	835	63	0.74	45.83 kN	40.81 kN	5.17 mm	7.88 mm	1.52	DL	
Stratford et al. [18]	1	Clay1	Clay masonry units	Static shear test	1200	1200	1	114.98 kN	104.44 kN	6.38 mm	14.02 mm	2.20	Sliding	
		Clay2		Static shear test	1200	1200	1	196.72 kN	74.1 kN	11.52 mm	12.1 mm	1.05	Detachment	
		Clay3		Static shear test	1200	1200	1	181.96 kN	166.28 kN	9.46 mm	10.2 mm	1.08	DT	
	2	Concrete1	Hollow Concrete masonry units	Static shear test	1200	1200	1	79.59 kN	59.36 kN	8.04 mm	12.46 mm	1.55	DT	
		Concrete2		Static shear test	1200	1200	1	105.02 kN	92.26 kN	7.24 mm	12.09 mm	1.67	DB	
		Concrete3		Static shear test	1200	1200	1	131.51 kN	110.47 kN	7.71 mm	12.22 mm	1.58	DT	
Al-Salloum and Al-Musallam [56]	1	IPL-C	URM	In-Plane Lateral Loading	1650	1450	0.87	125 kN	125 kN	0.8 mm	0.8 mm	1.00	Diagonal Sliding	
		IPL-S	Strengthened by GFRP laminate	In-Plane Lateral Loading	1650	1450	0.87	626 kN	510 kN	1.28 mm	1.3 mm	1.02	Detachment of laminates	
	2	IPV-C	URM	In-Plane Vertical Loading	1650	1450	0.87	445 kN	445 kN	0.6 mm	0.6 mm	1.00	Crushing	
		IPV-S	Strengthened by GFRP	In-Plane Vertical Loading	1650	1450	0.87	320 kN	280 kN	1.2 mm	1.3 mm	1.08	Detachment due to buckling	

6. Conclusions

In this paper, a literature review of the theoretical formulations used to predict the capacities of masonry walls retrofitted by GFRP materials subjected to in-plane and out-of-plane loading are reported. Furthermore, this study presents a manuscript aimed at a systematic review of the existing seismic retrofit/strengthening techniques by using GFRP for unreinforced masonry walls. A detailed anthology and organized review based on their common characteristics and effects on the seismic performance were described. According to the results of the studies:

- Despite the fact that in majority of cased retrofits were successful, Delamination and shear failure of the walls can suddenly occur without exploring all the potentialities of the strengthening material. Also, the increase in resistance was appreciable, in particular, in the case of the wall reinforced with diagonal GFRP strips as the delamination phenomenon is

avoided, in other term, failure mode of the strengthened masonry wall heavily depends on the local debonding.

- In the terms of Comparison of effectiveness of GFRP strips, it could be comprehended that the efficiency of combination of horizontal and vertical has more improvement in shear strength compare to diagonal configuration.
- Regarding horizontal and diagonal applications of GFRP strips and both of them, horizontal stripes have more effect on the improvement of shear capacity.
- Despite the fact that application of GFRP sheets on one side of the wall compared to both sides, is more realistic, makes the walls more prone and susceptible to out-of-plane deformation but provides better ductility.
- Throughout the review, almost in all of the studies application of GFRP materials compared to conventional materials like

Steel mesh, provide better post-peak behaviour and moderate decrease in load capacity and stiffness.

- In FRCM technique using cement as a mortar coating provides higher stiffness rather than lime. In stark contrast, however, using a lower cement ratio in coating mortar caused lower capacity of dissipation of energy.
- Regarding application of FRCM on one side of walls, prediction equations in designing guidelines codes, e.g., ACI, should be considered 30% reduced.

Conflict of interest

There is not conflict of interest.

References

- [1] Coburn, Andrew, and Robin Spence. Earthquake protection. John Wiley & Sons, 2003.
- [2] Figueiredo, A., H. Varum, A. Costa, D. Silveira, and C. Oliveira. "Seismic retrofitting solution of an adobe masonry wall." *Materials and Structures* 46, no. 1 (2013): 203-219.
- [3] Wang, Chuanlin, John P. Forth, Nikolaos Nikitas, and Vasilis Sarhosis. "Retrofitting of masonry walls by using a mortar joint technique: experiments and numerical validation." *Engineering Structures* 117 (2016): 58-70.
- [4] Ingham, Jason M., and Michael C. Griffith. "The performance of unreinforced masonry buildings in the 2010/2011 Canterbury earthquake swarm." Report to the Royal Commission of Inquiry (2011).
- [5] Gattesco, Natalino, and Ingrid Boem. "Out-of-plane behavior of reinforced masonry walls: Experimental and numerical study." *Composites Part B: Engineering* 128 (2017): 39-52.
- [6] Iuorio, Ornella, Jamiu A. Dauda, and [6] Paulo B. Lourenço. "Experimental evaluation of out-of-plane strength of masonry walls retrofitted with oriented strand board." *Construction and Building Materials* 269 (2021): 121358.
- [7] Mustafaraj, Enea, and Yavuz Yardim. "Retrofitting damaged unreinforced masonry using external shear strengthening techniques." *Journal of Building Engineering* 26 (2019): 100913.
- [8] Haach, Vladimir G., Graça Vasconcelos, and Paulo B. Lourenço. "Influence of aggregates grading and water/cement ratio in workability and hardened properties of mortars." *Construction and Building Materials* 25.6 (2011): 2980-2987.
- [9] Corradi, Marco, Antonio Borri, and Andrea Vignoli. "Strengthening techniques tested on masonry structures struck by the Umbria-Marche earthquake of 1997-1998." *Construction and building materials* 16.4 (2002): 229-239.
- [10] Capozucca, R., and E. Magagnini. "Experimental response of masonry walls in-plane loading strengthened with GFRP strips." *Composite Structures* 235 (2020): 111735.
- [11] Capozucca, Roberto. "Experimental FRP/SRP - historic masonry delamination." *Composite structures* 92.4 (2010): 891-903.
- [12] Walraven, J. C., and A. Q. C. van der Horst. *fib model code for concrete structures 2010*. International Federation for Structural Concrete (fib), 2013.
- [13] Drougkas, Anastasios, Pere Roca, and Climent Molins. "Numerical prediction of the behavior, strength and elasticity of masonry in compression." *Engineering Structures* 90 (2015): 15-28.
- [14] Drougkas, Anastasios, et al. "The confinement of mortar in masonry under compression: Experimental data and micro-mechanical analysis." *International Journal of Solids and Structures* 162 (2019): 105-120.
- [15] Capozucca, R., and V. Ricci. "Bond of GFRP strips on modern and historic brickwork masonry." *Composite structures* 140 (2016): 540-555.
- [16] Den Hartog, Jacob Pieter. *Advanced strength of materials*. Courier Corporation, 1987.
- [17] Capozucca, R. "Double-leaf masonry walls under in-plane loading strengthened with GFRP/SRG strips." *Engineering Structures* 128 (2016): 453-473.
- [18] Stratford, Tim, et al. "Shear strengthening masonry panels with sheet glass-fiber reinforced polymer." *Journal of Composites for Construction* 8.5 (2004): 434-443.
- [19] ACI (American Concrete Institute). "Design and construction guide of externally bonded FRCM systems for concrete and masonry repair and strengthening." (2013).
- [20] European Committee for Standardization (CEN). "EN 1052-3: Methods of test for masonry - Part 3: Determination of initial shear strength." (2007).
- [21] Triantafillou, Thanasis C. "Strengthening of masonry structures using epoxy-bonded FRP laminates." *Journal of composites for construction* 2.2 (1998): 96-104.
- [22] Eftekhar, Mohamad Reza, and Mehran Emami. "Investigation the Different Methods of Connecting GFRP Sheets to Ductility and In-Plane Behavior of Masonry Walls." *Journal Of Ferdowsi Civil Engineering* 31.2 (2018): 57-73.
- [23] Capozucca, R., and E. Magagnini. "Brickwork wall models strengthened with diagonal and horizontal GFRP strips." *Composite Structures* 271 (2021): 114062.
- [24] Capozucca, Roberto. "Experimental FRP/SRP - historic masonry delamination." *Composite structures* 92.4 (2010): 891-903.
- [25] Del Zoppo, Marta, et al. "In-plane shear capacity of tuff masonry walls with traditional and innovative Composite Reinforced Mortars (CRM)." *Construction and Building Materials* 210 (2019): 289-300.
- [26] ACI Committee 549, Guide to Design and Construction of Externally Bonded FRP Systems for Repair and Strengthening Concrete and Masonry Structures ACI 459.4 R13, American Concrete Institute, Farmington Hills, MI, 2013.
- [27] Antonietta, AIELLO Maria, et al. "Istruzioni per la Progettazione, l'Esecuzione ed il Controllo di Interventi di Consolidamento Statico mediante l' utilizzo di Compositi Fibrorinforzati Materiali, strutture di ca e di cap, strutture murarie CNR-DT 200 R1/2013." (2013): 1-168.
- [28] Yu, Piyong, Pedro Silva, and Antonio Nanni. "In-plane performance of unreinforced concrete masonry strengthened with prestressed GFRP bars." *Journal of Composites for Construction* 21.1 (2017): 04016064.
- [29] Yu, Piyong, Pedro Franco Silva, and Antonio Nanni. "Innovative mechanical device for the post-tensioning of glass fiber reinforced polymer bars for masonry type retrofit applications." *Experimental mechanics* 44.3 (2004): 272-277.
- [30] De Lorenzis, Laura, Antonio Nanni, and Antonio La Tegola. "Bond of near surface mounted FRP rods in concrete masonry units." *The Seventh Annual International Conference on Composites Engineering (ICCE/7)*, Denver, Colorado, 2000.
- [31] Essawy, Ahmed S., and Robert G. Drysdale. "Macroscopic failure criterion for masonry assemblages." *Proc., 4th Canadian Masonry Symp.* Vol. 1. 1986.
- [32] Wang, Q., Z. Chai, Y. Huang, Y. Yang, and Y. Zhang. "Seismic shear capacity of brick masonry wall reinforced by GFRP." (2006): 563-580.
- [33] Yi, T., et al. "Flange effects on the nonlinear behaviour of URM piers." *The Masonry Society Journal* 26.2 (2008): 31-42.
- [34] Yi, T., F. L. Moon, and R. T. Leon. "Effective pier model for the nonlinear in-plane analysis of individual URM piers." (2005): 21-35.
- [35] Russell, A. P., and J. M. Ingham. "The influence of flanges on the in-plane seismic performance of URM walls in New Zealand buildings." *NZSEE Conference*, Wellington, New Zealand, 2010.
- [36] FEMA 356. *Prestandard and commentary for the seismic rehabilitation of buildings*. Applied Technology Council (ATC). Washington, DC; 2000.
- [37] Researching Group of Seismic Design Code on Brick Masonry Structure., *Shear strength of unreinforced brick masonry wall*, J. Building Structures, No. 6, 5(1984) 1- 12 (in Chinese).
- [38] Gostič, S., A. Mezgec, and R. Žarnić. "Študija učinkovitosti naprednih metod za sanacijo zidanih stavb." *Raziskovalni projekt MŠZŠ Z2-3411* (2004).
- [39] Borri, Antonio, et al. "Reinforcement of historic masonry with high strength steel cords." *Masonry International* 23.3 (2010): 79-90.

- [40] Borri, Antonio, et al. "Masonry wall panels with GFRP and steel-cord strengthening subjected to cyclic shear: An experimental study." *Construction and Building Materials* 56 (2014): 63-73.
- [41] Gattesco, Natalino, and Ingrid Boem. "Experimental and analytical study to evaluate the effectiveness of an inplane reinforcement for masonry walls using GFRP meshes." *Construction and Building Materials* 88 (2015): 94-104.
- [42] Gattesco, Natalino, Claudio Amadio, and Chiara Bedon. "Experimental and numerical study on the shear behavior of stone masonry walls strengthened with GFRP reinforced mortar coating and steel-cord reinforced repointing." *Engineering Structures* 90 (2015): 143-157.
- [43] Borri, Antonio, et al. "Masonry wall panels retrofitted with thermal-insulating GFRP-reinforced jacketing." *Materials and Structures* 49.10 (2016): 3957-3968.
- [44] Ashraf, Mohammad, et al. "Seismic behavior of unreinforced and confined brick masonry walls before and after ferrocement overlay retrofitting." *International Journal of Architectural Heritage* 6.6 (2012): 665-688.
- [45] Mustafaraj, Enea, and Yavuz Yardim. "In-plane shear strengthening of unreinforced masonry walls using GFRP jacketing." *Periodica Polytechnica Civil Engineering* 62.2 (2018): 330-336.
- [46] Weng, Dagen, et al. "Experimental study on seismic retrofitting of masonry walls using GFRP." *Proceedings of 13th World Conference on Earthquake Engineering*. 2004.
- [47] Nezhad, Razieh Sistani, and Mohammad Z. Kabir. "Experimental investigation on out-of-plane behavior of GFRP retrofitted masonry panels." *Construction and Building Materials* 131 (2017): 630-640.
- [48] Gattesco, Natalino, and Ingrid Boem. "Out-of-plane behavior of reinforced masonry walls: Experimental and numerical study." *Composites Part B: Engineering* 128 (2017): 39-52.
- [49] Dong, Zhifang, et al. "Out-of-plane strengthening of unreinforced masonry walls using textile reinforced mortar added short polyvinyl alcohol fibers." *Construction and Building Materials* 260 (2020): 119910.
- [50] Abdulsalam, Bahira, et al. "Behavior of GFRP strengthening masonry walls using glass fiber composite anchors." *Structures*. Vol. 29. Elsevier, 2021.
- [51] Tumialan, J. Gustavo, Nestore Galati, and Antonio Nanni. "FRP strengthening of UMR walls subject to out-ofplane loads." *ACI Structures Journal* 100.3 (2003): 312-329.
- [52] Tumialan, J. Gustavo, Nestore Galati, and Antonio Nanni. "Field assessment of unreinforced masonry walls strengthened with fiber reinforced polymer laminates." *Journal of Structural engineering* 129.8 (2003): 1047-1056.
- [53] Sadek, H., and S. Lissel. "Seismic performance of masonry walls with GFRP and Geogrid Bed joint reinforcement." *Construction and Building Materials* 41 (2013): 977-989.
- [54] El-Diasity, Mosaad, et al. "Structural performance of confined masonry walls retrofitted using ferrocement and GFRP under in-plane cyclic loading." *Engineering Structures* 94 (2015): 54-69.
- [55] Alsayed, Saleh H., et al. "Blast response of GFRP-strengthened infill masonry walls." *Construction and building materials* 115 (2016): 438-451.
- [56] Al-Salloum, Yousef A., and Tarek H. Almusallam. "Load capacity of concrete masonry block walls strengthened with epoxy-bonded GFRP sheets." *Journal of composite materials* 39.19 (2005): 1719-1745.



This is an open-access article under a [Creative Commons Attribution 4.0 International License](https://creativecommons.org/licenses/by/4.0/).